4x4 Hybrid Electric Vehicle vs. Fully Electric Vehicle Mobility in Drastically Changing Terrain Conditions

Jesse Paldan¹, Vladimir Vantsevich¹, David Gorsich², Michael Letherwood³

¹ University of Alabama at Birmingham
 ² U.S. Army Ground Vehicle Systems Center
 ³ Alion Science & Technology

Abstract. Active driveline technologies allow vehicles to dynamically control power distribution among driving wheels to improve vehicle operational parameters that impact terrain mobility. Two 4x4 electrified drivelines are compared which provide a variable power split: a hybrid electric vehicle with a controllable power transmitting unit and a fully electric vehicle (FEV) with individual electric wheel drives. The individual e-drives have the potential to improve mobility when the left and right wheel terrain conditions are drastically different.

Keywords: Vehicle Dynamics, Vehicle Mobility, Hybrid and Electric Vehicles

1 Introduction

The circumferential forces of driving wheels, which determines wheel traction, are dependent on the power distribution methods used in the driveline system. With different power transmitting units, the driving wheels receive different force distributions which has important effects on the vehicle's operational performance, including mobility. FEVs have used individual motor control for enhancing safety, comfort, and handling dynamics [1]. Individual wheel power distribution algorithms have been studied for use in off-road vehicles to improve traction while reducing power loss and soil damage [2]. On terrain, different wheels can experience very different conditions as the vehicle moves over uneven soil of varying quality, resulting in the wheels having different traction capability and tire slippages. The slippage s_{δ} is defined as the loss of linear velocity V_{r}

$$s_{\delta i}^{\prime(\prime\prime)} = 1 - \frac{V_x}{V_{ti}^{\prime(\prime\prime)}}, i = 1, n$$
 (1)

Where ' and '' refer to the right and left wheels, respectively, of driving axle i on a vehicle with n driving axles. $V_{ti}^{\prime(\prime\prime)}$ is the theoretical velocity of the wheel without slip defined in Eq. (2) as

$$V_{ti}^{\prime(\prime\prime)} = \omega_{wi}^{\prime(\prime\prime)} r_{wi}^{0\prime(\prime\prime)}, i = 1, n$$
 (2)

where $r_w^{0'(\prime\prime)}$ is the rolling radius in the driven mode, at no applied torque, used as the reference for zero slip.

However, even without slip, if the total resistance is close to zero, the vehicle still can have a difference in velocity from the theoretical velocity. Tire radii $r_w^{0'(\prime\prime)}$ are not necessarily the same because of differing normal loads, inflation pressures, tire sizes, etc. At the same time, the wheels all move together at even linear velocity, giving the vehicle a theoretical linear velocity of V_a . Velocity V_a is defined as

$$V_a = \omega_0 r_a^0 \tag{3}$$

where r_a^0 is the generalized rolling radius of the vehicle in the driven mode, reduced to the input shaft of the transfer case. That is, the theoretical velocity is the linear velocity of an equivalent single wheel with rotational velocity ω_0 and rolling radius in the driven mode r_a^0 , where, ω_0 is the angular velocity of the input shaft.

When V_{ti} and V_a differ, a kinematic discrepancy factor, m_{Hi} , exists, defined in a form similar to the tire slippage as

$$m_{Hi}^{\prime(\prime\prime)} = \frac{V_{ti}^{\prime(\prime\prime)} - V_a}{V_{ti}^{\prime(\prime\prime)}}, i = 1, n \tag{4}$$

The kinematic discrepancy factor is the slippage of a tire that is caused by the difference in the velocities $V_{ti}^{\prime(\prime\prime)}$ and V_a of the vehicle in the driven mode when the resistance to motion is close to zero. m_{Hi} can be either positive or negative, meaning that some of the wheels may slip or skid. The presence of slippage results in the vehicle's linear velocity decrease from V_a to V_x which can be characterized by a generalized slippage of the vehicle [3] as

$$s_{\delta a} = \frac{v_a - v_x}{v_a} \tag{5}$$

By comparing the velocity terms in Eqs. (1) and (5) with the kinematic discrepancy in Eq. (4), it can be found that

$$s_{\delta i}^{\prime(\prime\prime)} = m_{Hi}^{\prime(\prime\prime)} + \left(1 - m_{Hi}^{\prime(\prime\prime)}\right) s_{\delta a}, i = 1, n \tag{6}$$

Eq. (6) shows that kinematic discrepancies affect the distribution of tire slippages and the overall velocity loss of the vehicle. By using different power transmitting units in the driveline of a 4x4 hybrid electric vehicle (HEV), these kinematic discrepancies can be made different, however, the gear ratios in the driveline are usually fixed. By using active power transmitting units or individual wheel motors in a 4x4 FEV, a variable gear ratio may be introduced, allowing real time control over factors m_{Hi} and the radius r_a^0 . Two such methods, i.e. HEV and FEV, are compared in this paper for a condition in which a vehicle moves with drastically different terrain conditions under each wheel.

2 Two 4x4 Driveline Models with Controllable Power Split

Two driveline models are considered here, including a hybrid electric (HE) driveline with a controllable power transmitting unit and a FEV with individual wheel motors. Both vehicles are capable of controlling the wheel power split where the HE driveline has a controllable front/rear power split while the FEV with individual motors is also capable of controlling the left/right split.

2.1 Vehicle with Hybrid Electric-Power Transmitting Unit (HE-PTU)

The hybrid electric vehicle is a series hybrid with a single traction motor. Electrical power is supplied by the high voltage battery, which is charged by the engine/generator set. Figure 1 shows the driveline with all torques (T), angular velocities (ω) , and gear reduction ratios (u) labeled.

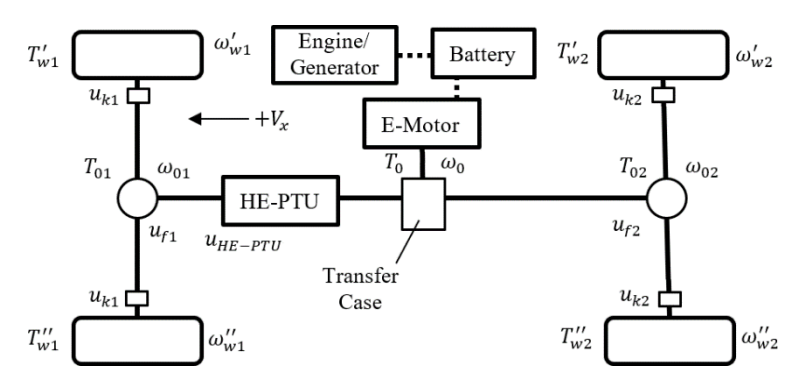


Figure 1. Hybrid electric driveline with HE-PTU

The transfer case interaxle differential transits mechanical power from the e-motor to the front and rear axles through final drive gear ratios u_{f1} and u_{f2} . u_{ki} are the gear ratios of the wheel-hub gear sets, usually the same for the left and right wheels of an axle, and interwheel open differentials transmit power to the left and right wheels of an axle. The controllable power split is performed through the addition of a HE-PTU installed between the transfer case and front axle [4].

The internal mechanism of the HE-PTU is shown in Figure 2a, and its location in the vehicle in Figure 2b. The HE-PTU employs a planetary gear set, in which one of its three connections is the input from the transfer case and the second is the output to the front axle differential. On the third connection is an eddy-current brake capable of applying a torque to the ring gear shaft. With the third element locked, the gear ratio between the input and output is 1+K, where K is the ratio of the number of teeth on the ring gear to that of the sun gear. Therefore, the braking torque required to fully stop the ring gear, T_B^{max} , corresponds to maximum gear ratio $u_{HE-PTU}^{max} = (1+K)$.

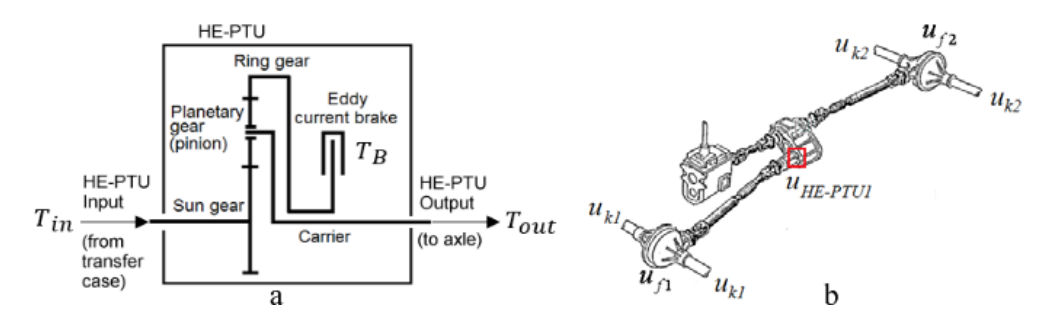


Figure 2. a) HE-PTU internal diagram and b) HE-PTU location on vehicle

As the braking torque is released, the gear ratio drops. This variable gear ratio u_{HE-PTU} is expressed by Eq. (7) in terms of the input, output, and brake torques T_{in} , T_{out} , and T_b as

$$u_{HE-PTU} = u_{HE-PTU}^{max} \frac{T_{B}}{T_{B}^{max}} = \frac{(1+K)}{K} \frac{T_{B}}{T_{in}} = \frac{(1+K)^{2}}{K} \frac{T_{B}}{T_{out}}$$
(7)

The kinematic discrepancies are [3]

$$m_{Hi}^{\prime(\prime\prime)} = 1 - \frac{u_{ki}u_i^{\prime(\prime\prime)}}{r_{wi}^{o'(\prime\prime)}}r_a^0, i = 1, n$$
 (8)

The size of radius r_a^0 can be calculated from the tire longitudinal stiffness factor K_{xi} , gear ratios u_i , and r_{wi}^0 as

$$r_a^0 = \left(\sum_{i=1}^n K_{xi}^{\prime(i)} r_{wi}^{0\prime(i)} / u_{ki} u_i^{\prime(i)}\right) \left(\sum_{i=1}^n K_{xi}^{\prime(i)}\right)^{-1} \tag{9}$$

Since Eq. (8) and Eq. (9) have a dependency on u_i , the kinematic discrepancy can be controlled by adjusting u_{HE-PTU} , which provides an additional multiplier on ratio u_1 .

2.2 FE Vehicle with Individual Wheel Drives

In the FEV, the single motor is replaced with four smaller motors, one dedicated to each wheel (Figure 3). Management of wheel power distribution is performed by individual control of each wheel. Ratios $u_i^{\prime(\prime\prime)}$ are replaced with control signals, where

$$\omega_{wi}^{\prime(n)} = \omega_0 / u_i^{\prime(n)} \tag{10}$$

In a fully electric (FE) driveline, the transfer case, whose output shaft has angular velocity ω_0 , is not present. However, the quantity ω_0 can be understood as a virtual quantity relating to the overall drop in linear velocity resulting from slippage when the vehicle's actual linear velocity V_x is compared to the theoretical velocity calculated from $V_a = \omega_0 r_a^0$ (see Eq. (3)).

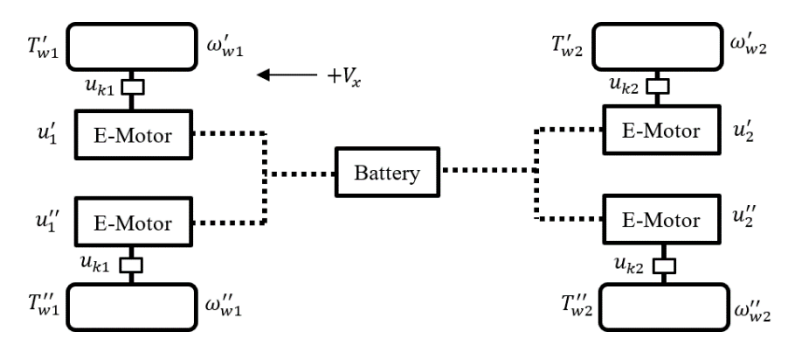


Figure 3. Fully electric driveline with individual wheel motors

This fact allows the signals $u_i^{\prime(\prime\prime)}$ to be treated as part of a "virtual driveline" connecting the wheel shafts through a computer code. This vehicle configuration has four kinematic discrepancies, controllable through the combination of all four values of $u_i^{\prime(\prime\prime)}$ as shown in Eq. (11)

$$m_{Hi}^{\prime(\prime\prime)} = 1 - \frac{u_i^{\prime(\prime\prime)}}{r_{wi}^{0\prime(\prime\prime)}} r_a^0 = 1 - \frac{u_i^{\prime(\prime\prime)}}{r_{wi}^{0\prime(\prime\prime)}} \frac{\sum_{l=1}^n K_{xi} r_{wi}^{0\prime(\prime\prime)} / u_i^{\prime(\prime\prime)}}{\sum_{l=1}^n K_{xi}}, \quad i = 1, n$$
 (11)

3 Mobility in Drastically Differing Terrain Condition

At the wheel's tire-terrain contact, the terrain condition under the tire plays an important role in the traction force that the wheel may develop. A portion of the magnitude of the normal reaction is utilized in generating the circumferential wheel force needed for motion where this ratio is the current friction coefficient μ_x [3]

$$\mu_x = F_x / R_z \tag{12}$$

The maximum circumferential wheel force that can be attained in the contact between the wheel and the surface of motion, F_x^{max} is [3]

$$F_x^{max} = \mu_{nx} R_z \tag{13}$$

where μ_{px} is the peak friction coefficient, related to the tire slippage in Eq. (14) as

$$F_{xi}^{'('')} = \mu_{xi}^{'('')} R_{zi}^{'('')} = \mu_{pxi}^{'('')} R_{zi}^{'('')} \left(1 - \frac{s_{\delta c}^{'('')}}{2s_{\delta}^{'('')}} \left(1 - e^{\frac{-2s_{\delta c}^{'('')}}{s_{\delta c}^{'('')}}}\right)\right) i = 1, n$$
(14)

where R_z is the normal reaction and $s_{\delta c}$ is the tire characteristic slippage [5]. Peak friction therefore defines the maximum traction and affects the shape of the traction/slippage curve. Peak friction can change with factors such as soil quality, compaction, moisture content, etc. A stochastic model of the peak friction coefficient is used to characterize the terrain condition. The soil condition can be different under each of the wheel tracks, as shown in Figure 4.

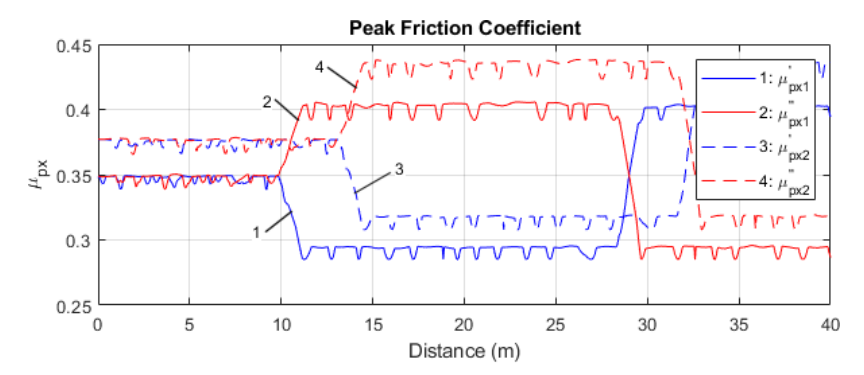


Figure 4. Peak Friction Coefficient

Here, the terrain starts off having close values of the peak friction coefficients under the left and right tires with only small variations. At 13 to 15 m of travel, the vehicle encounters a patch of terrain in which the right and left wheels are on different conditions. The front wheels compact the soil, giving different μ_{px} values for the rear wheels' pass as shown by the dotted line curves. Between 28-33 m, the side with the better terrain condition switches. This terrain profile was composited to test the effect of drastically different mobility conditions of the two vehicle driveline models.

The variable gear ratios u_1 (for the HEV) and $u_i^{\prime\prime\prime}$ (for the individual drives) were computed for both drivelines by optimizing the ratio V_x/V_{a*} , where V_{a*} is the theoretical velocity with all ratios held constant and equal to $u_i^{\prime\prime\prime} = u_{fi}u_{ki}$ [6]. Figure 5 illustrates the variable gear ratios of the HE and FE drives on the same vehicle.

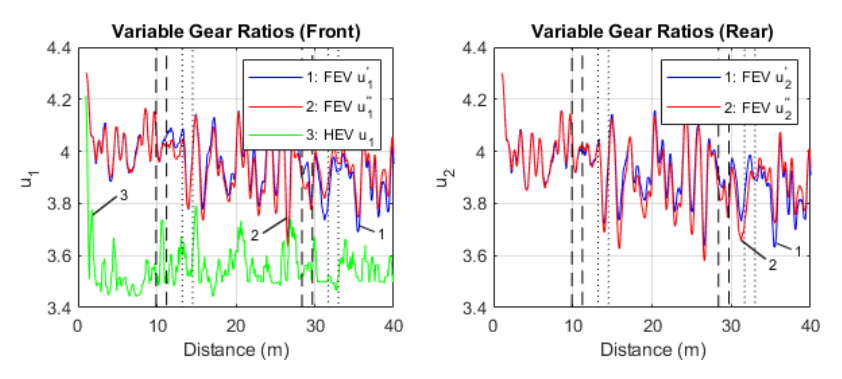


Figure 5. Variable gear ratios of hybrid electric and fully electric drivelines

Dashed and dotted lines mark where the front and rear tires reach the start and end of terrain transitions, respectively. The HE driveline, which cannot separately control power between the left and right sides, does not change in its overall pattern after the terrain transitions. For the FE driveline, the left and right gear ratios are close before the terrain split. After the split, the gear ratios u_i' of the right side, with the lower values

of μ_{pxi} , increase above $u_i^{''}$. $u_i^{'}$ and $u_i^{''}$ swap positions after the second terrain change to keep the vehicle moving with the same mobility. Figure 6 is the linear velocity of the same 9.8 ton-vehicle with both drivelines when the variable gear ratios shown in Figure 5 are applied. The velocities of the same vehicle with the gear ratios held constant are also plotted. The HE driveline has a more consistent, but overall lower velocity. When the split terrain condition is reached, the vehicle with HE driveline loses mobility and its velocity drops. The FE driveline does not lose velocity on the split terrain, but the variation of the velocity is higher. The second transition at 28-33 m of travel did not impact the velocity of the vehicle with either the HE of FE driveline.

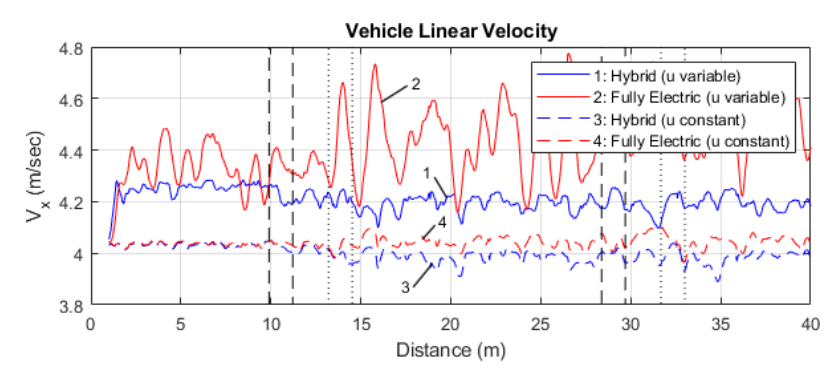


Figure 6. Comparison of velocity vs. travel distance for the vehicle with HE and FE drivelines

Table 1 provides a numeric comparison of the mean velocity of the vehicle before and after the terrain split. Applying variable gear ratios to both drivelines always improves vehicle velocity compared to the same driveline under constant values of the gear ratios. After the terrain split, the HEV's improvement drops slightly, from 5.4% to 5.2%, while the FEV's improvement increases from 7.1% to 10.3%. Going from even terrain to the split terrain, the HEV with a variable gear ratio has a drop in velocity of 1.2%, while the FEV's velocity increases by 3.3%.

Table 1. Mean velocity (in m/sec) before and after the first terrain transition.

	HE Driveline	HE Driveline	FE Driveline	FE Driveline
	(Constant u)	(Variable u)	(Constant u)	(Variable u)
Before (0-10 m)	4.0320	4.2513	4.0357	4.3228
After (15-40 m)	3.9854	4.1926	4.0458	4.4633

Figure 7 is a plot of the vehicle's generalized slippage and rolling radius in the driven mode. Higher r_a^0 leads to an increase in theoretical velocity V_a (Eq. (3)), while higher V_a and lower slippage correspond to higher actual velocity V_x (Eq. (5)). The higher slippage results in a velocity loss of the HE vehicle. r_a^0 increases and $s_{\delta a}$ drops in the split terrain for the fully electric vehicle and its' ability to take advantage of good traction conditions of the wheels on one side outweighs the effect of the poor traction side, even though the gain and loss in $\mu_{pxi}^{\prime(\prime\prime)}$ are balanced at both sides.

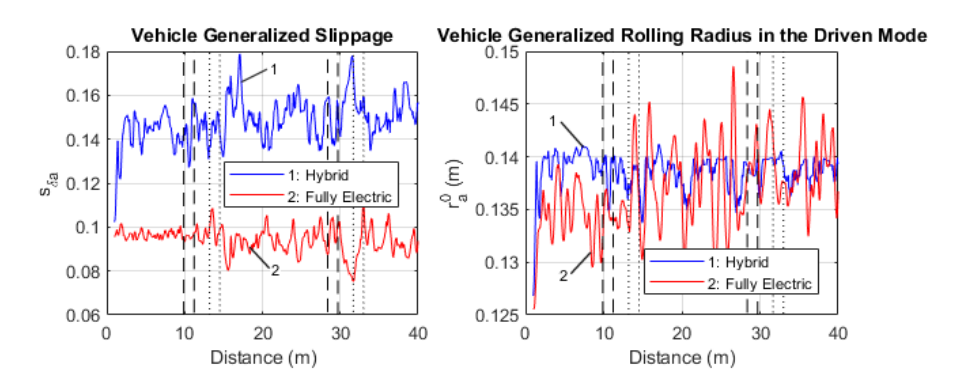


Figure 7. Vehicle generalized slippage and rolling radius in the driven mode

4 Conclusion

The operational mobility performance of a 4x4 vehicle capable of controlling the front/rear power split by using the HE-PTU was compared to that of a vehicle capable of individual e-drive of each wheel. When the left and right wheel conditions are drastically different, adjusting the left/right power balance can improve mobility, allowing faster velocity on the same terrain split condition. With variable gear ratios, the FE driveline increased the vehicle's velocity by 10.3% compared to 5.2% with the HE driveline.

Acknowledgments This research funded by the US Army CCDC Ground Vehicle Systems Center and partially by the National Science Foundation (award IIS-1849264).

5 References

- Kanchwala, H., Rodriguez, P., Mantaras, D., Wideberg, J. et al:, "Obtaining Desired Vehicle Dynamics Characteristics with Independently Controlled In-Wheel Motors: State of Art Review," SAE Int. J. Passeng. Cars - Mech. Syst. 10(2):413-425, 2017.
- Shukhman, S.. Malyarevich, V.:, "AWD Vehicle with Individual Wheel Input Power Control: Dynamics and Ecological Properties Improvement," SAE Technical Paper 2010-01-1897, 2010.
- 3. Andreev, A. F., Kabanau, V. I., Vantsevich, V. V.: "Driveline Systems of Ground Vehicles-Theory and Design", Taylor & Francis Group, Boca Raton, London and New York (2010).
- Vantsevich, V.V., Paldan, J., Gray, J.P., "A Hybrid-Electric Power Transmitting Unit for 4x4 Vehicle Applications: Modeling and Simulation", ASME 2014 Dynamic Systems and Control Conference, San Antonio, Texas, USA, 2014.
- Andreev, A. F., Vantsevich, V. V.: "Tyre and Soil Contribution to Tyre Traction Characteristic", IAVSD 2017 International Symposium on Vehicle Dynamics, Paper #206, Rockhampton, Australia, August 14-18, 2017
- Vantsevich, V., Gorsich, D., Paldan, J., and Letherwood, M., "A Virtual Driveline Concept to Maximize Mobility Performance of Autonomous Electric Vehicles," SAE Technical Paper 2020-01-0746, 2020 (in publication).